Acoustic Localisation of Coronary Artery Disease

Simon Shaw

people.brunel.ac.uk/~icsrsss

BICOM, *The Brunel Institute of Computational Mathematics Brunel University, Uxbridge UB8 3PH, England*

Contents

Image Credits: google images; SE Greenwald, www.bbc.co.uk

PDE's with memory: viscoelasticity back

Viscoelasticity

PDE's with memory

back

Main themes

- Viscoelastic materials exhibit memory

Details

Application areas:

- damping (polymers)
- structures (concrete)
- porous media (geomechanics)
- electromagnetics (Debye media)
- non-Fickian diffusion
- soft tissue biomechanics

Main themes

- Viscoelastic materials exhibit memory
- which manifests as:
  - creep

Details

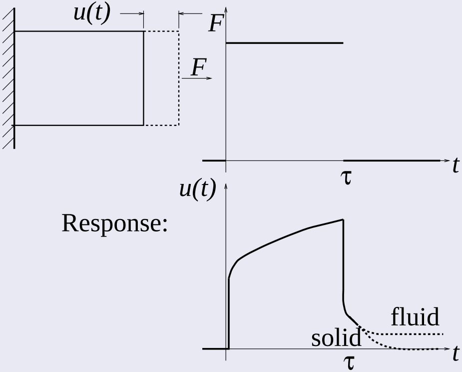

Main themes

- Viscoelastic materials exhibit memory
- which manifests as:
  - creep
  - relaxation

Details

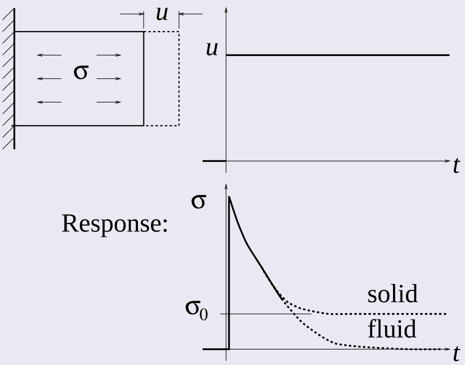

Main themes

- Viscoelastic materials exhibit memory
- which manifests as:
  - creep
  - relaxation
  - hysteresis

Details

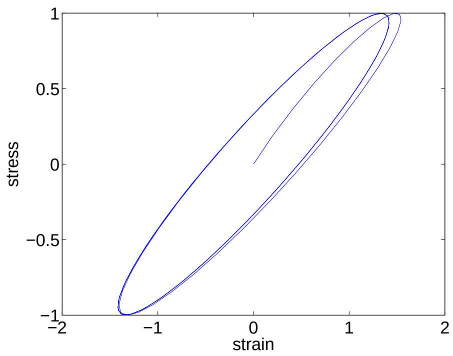

Main themes

- Viscoelastic materials exhibit memory
- which manifests as:
  - creep
  - relaxation
  - hysteresis
  - frequency dependence

Details

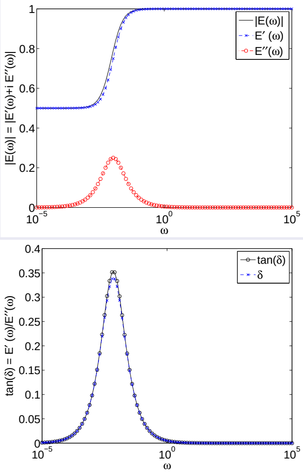

Main themes

- Viscoelastic materials exhibit memory
- which manifests as:
  - creep
  - relaxation
  - hysteresis
  - frequency dependence
- Typically described by partial differential equations with either
  - internal variables
  - or memory

Details

$$u_{tt} - \nabla^2 u = f - \nabla \cdot \sigma$$

$$\sigma_t + \gamma\sigma = \mu \nabla u$$

$$u_{tt} - \nabla^2 u = f - \int_0^t b(t-s)\nabla^2 u(s)\, ds$$

Prony: $\qquad b(t) = \sum_i b_i e^{-t/\tau_i}$

or weakly singular: t^p

or fractional calculus

nonlinearity, e.g. $\gamma \leftarrow \gamma(u)$

Main themes

- Viscoelastic materials exhibit memory
- which manifests as:
    - creep
    - relaxation
    - hysteresis
    - frequency dependence
- Typically described by partial differential equations with either
    - internal variables
    - or memory

Details

$$u_{tt} - \nabla^2 u = f - \nabla \cdot \sigma$$

$$\sigma_t + \gamma\sigma = \mu \nabla u$$

$$u_{tt} - \nabla^2 u = f - \int_0^t b(t-s)\nabla^2 u(s)\, ds$$

Prony: $\qquad b(t) = \sum_i b_i e^{-t/\tau_i}$

or weakly singular: t^p

or fractional calculus

nonlinearity, e.g. $\gamma \leftarrow \gamma(u)$

Analysis can exploit the fading memory: an example. . .

Maxwell's equations — dispersive dielectrics

$$\begin{aligned} \nabla \times \boldsymbol{E} + \dot{\boldsymbol{B}} &= 0 & \qquad \nabla \cdot \boldsymbol{B} &= 0 \\ \nabla \times \boldsymbol{H} - \dot{\boldsymbol{D}} &= \boldsymbol{J} & \qquad \nabla \cdot \boldsymbol{D} &= \varrho \end{aligned}$$

What has this got to do with viscoelasticity? Dispersion...

Maxwell's equations — dispersive dielectrics

$$\begin{aligned} \nabla \times \boldsymbol{E} + \dot{\boldsymbol{B}} &= 0 & \qquad \nabla \cdot \boldsymbol{B} &= 0 \\ \nabla \times \boldsymbol{H} - \dot{\boldsymbol{D}} &= \boldsymbol{J} & \qquad \nabla \cdot \boldsymbol{D} &= \varrho \end{aligned}$$

What has this got to do with viscoelasticity? Dispersion. . .

$\boldsymbol{B} = \mu \boldsymbol{H}$ but dielectric polarization is not instantaneous. . .

Debye: $\boldsymbol{D} = \varepsilon_0(1+\chi)\boldsymbol{E} + \boldsymbol{P}$ with $\tau\dot{\boldsymbol{P}} + \boldsymbol{P} = (\varepsilon_s - \varepsilon_\infty)\varepsilon_0 \boldsymbol{E}$

with $\boldsymbol{P}(0) = \mathbf{0}$ and the ε's known. Hence, we can use either of. . .

$$(\varepsilon_0\varepsilon_\infty)^{-1}\boldsymbol{D} = \boldsymbol{E} + \dot{\psi} * \boldsymbol{E} \qquad \text{or} \qquad \varepsilon_0\varepsilon_\infty \boldsymbol{E} = \boldsymbol{D} + \dot{\varphi} * \boldsymbol{D}$$

which is viscoelasticity! Exploit related results. . .

Example of *a priori* control. No Gronwall!

Find $\boldsymbol{D}$ such that: $\ddot{\boldsymbol{D}} + \nabla \times \mu^{-1} \nabla \times \boldsymbol{E} + \sigma \dot{\boldsymbol{E}} = -\dot{\boldsymbol{J}}_a,$

where $\varepsilon \dot{\boldsymbol{E}}(t) = \dot{\boldsymbol{D}}(t) + \varphi'(t) \boldsymbol{D}(0) - \int_0^t \varphi_s(t-s) \dot{\boldsymbol{D}}(s)\, ds.$

Theorem

With $\boldsymbol{G}(t) = -\dot{\boldsymbol{J}}_a(t) - \sigma \varepsilon^{-1} \varphi'(t) \boldsymbol{D}(0)$ *known and if* $\sigma > 0$ *we have,*

$$\mu\varepsilon \|\dot{\boldsymbol{D}}(t)\|_0^2 + \check{\varphi} \|\nabla \times \boldsymbol{D}(t)\|_0^2 + \mu\sigma\check{\varphi} \|\dot{\boldsymbol{D}}\|^2_{L_2(0,t;\boldsymbol{L}_2(\Omega))}$$
$$\leqslant \mu\varepsilon \|\dot{\boldsymbol{D}}(0)\|_0^2 + \|\nabla \times \boldsymbol{D}(0)\|_0^2 + \frac{\mu\varepsilon^2}{\sigma\check{\varphi}} \|\boldsymbol{G}\|^2_{L_2(0,t;\boldsymbol{L}_2(\Omega))}.$$

Remark: similar results are possible if $\sigma = 0$.

Using also Rivera & Menzala's lemma (Quart. Appl. Math., LVII, 1999)

Example: a discrete abstract wave equation

Relaxation (fading memory) expressed through internal variable rate equations: find $\boldsymbol{u}\colon I \to V$ such that,

$$(\varrho\ddot{\boldsymbol{u}}(t),\boldsymbol{v}) + a(\boldsymbol{u}(t),\boldsymbol{v}) + b(\dot{\boldsymbol{u}}(t),\boldsymbol{v}) = \langle L(t),\boldsymbol{v}\rangle + \sum_{q=1}^{N_\varphi} a(\boldsymbol{u}_q^\star(t),\boldsymbol{v}) \ \forall \boldsymbol{v}\in V,$$

$$a(\tau_q\dot{\boldsymbol{u}}_q^\star(t) + \boldsymbol{u}_q^\star(t),\boldsymbol{v}) = a(\varphi_q\boldsymbol{u}(t),\boldsymbol{v}) \text{ for } q = 1,\ldots,N_\varphi,\ \forall \boldsymbol{v}\in V.$$

And its DG-in-time approximation: find $(U,W)\approx(u,\dot{u})$ such that

$$\left(\!\left(\varrho\dot{W},\vartheta\right)\!\right)_n + (\varrho\,[\![W]\!]_{n-1},\vartheta_{n-1}^+) + a\left(\!\left(U,\vartheta\right)\!\right)_n + b\left(\!\left(W,\vartheta\right)\!\right)_n - \sum_{q=1}^{N_\varphi} a\left(\!\left(Z_q,\vartheta\right)\!\right)_n = \langle\!\langle L,\vartheta\rangle\!\rangle_n$$

$$a\left(\!\left(\dot{U}-W,\zeta\right)\!\right)_n + a([\![U]\!]_{n-1},\zeta_{n-1}^+) = 0,$$

$$\text{for } q=1,\ldots,N_\varphi \qquad a\left(\!\left(\tau_q\dot{Z}_q + Z_q - \varphi_q U,\xi_q\right)\!\right)_n + a(\tau_q\,[\![Z_q]\!]_{n-1},\xi_{q,n-1}^+) = 0,$$

for all test functions θ, ζ, $\xi_1,\ldots\in\mathbb{P}_r(I_n;V^h)$.

Sharp discrete stability

The discrete scheme. . .

$$\left(\!\left(\varrho\dot{W},\vartheta\right)\!\right)_n + (\varrho\,[\![W]\!]_{n-1}\,,\vartheta_{n-1}^{+}) + a\left(\!\left(U,\vartheta\right)\!\right)_n + b\left(\!\left(W,\vartheta\right)\!\right)_n - \sum_{q=1}^{N_\varphi} a\left(\!\left(Z_q,\vartheta\right)\!\right)_n = \langle\!\langle L,\vartheta\rangle\!\rangle_n$$

$$a\left(\!\left(\dot{U}-W,\zeta\right)\!\right)_n + a([\![U]\!]_{n-1}\,,\zeta_{n-1}^{+}) = 0,$$

$$\text{for } q=1,\dots,N_\varphi \qquad a\left(\!\left(\tau_q\dot{Z}_q + Z_q - \varphi_q U,\xi_q\right)\!\right)_n + a(\tau_q\,[\![Z_q]\!]_{n-1}\,,\xi_{q,n-1}^{+}) = 0,$$

satisfies, for each time t_m,

$$\|\varrho^{1/2}W_m^-\|_0^2+\|\varphi_0^{1/2}U_m^-\|_V^2+\sum_{q=1}^{N_\varphi}\left\|\frac{Z_{q,m}^- - \varphi_q U_m^-}{\sqrt{\varphi_q}}\right\|_V^2+2\int_0^{t_m}\left(\sum_{q=1}^{N_\varphi}\left\|\frac{Z_q-\varphi_q U}{\sqrt{\tau_q\varphi_q}}\right\|_V^2 + b(W,W)\right)dt$$

$$+\sum_{n=1}^{m}\left(\sum_{q=1}^{N_\varphi}\left\|\left[\!\!\left[\frac{Z_q-\varphi_q U}{\sqrt{\varphi_q}}\right]\!\!\right]_{n-1}\right\|_V^2 + \|\varrho^{1/2}\,[\![W]\!]_{n-1}\,\|_0^2 + \|\varphi_0^{1/2}\,[\![U]\!]_{n-1}\,\|_V^2\right)$$

$$= 2\int_0^{t_m}\langle L,W\rangle\,dt + \|\varrho^{1/2}W_0^-\|_0^2 + \|\varphi_0^{1/2}U_0^-\|_V^2.$$

Leads to Non-Gronwall discrete stability. (Error bounds?)

Coronary Artery Disease

back

Coronary Artery Disease

back

Coronary Artery Disease (CAD)

- In the UK in 2010 CAD caused over 14% of all deaths (80,568/561,666).
  - About 95% in people aged 55+ yrs.
- €7.5 billion — approx 2009 cost...
  - €2 billion — healthcare (*per capita* €32)
  - €3.5 billion — lost productivity
  - €2 billion — informal patient care
- An expensive killer — huge tax burden.
- Poor diet & ageing population will exacerbate problem.

Source: *Tables 6.2, 6.3, Coronary Heart Disease Statistics. A compendium of health statistics. 2012 ed. British Heart Foundation. ISBN 978-1-899088-12-6*

What is Coronary Artery Disease?

- Lipids & calcium deposits form atheromatous plaques between endothelium and artery wall
- Stenosis grows and reduces artery calibre.
- Vulnerable plaque suddenly ruptures — causes clot
- *Myocardial Ischaemia/Infarction*: a 'heart attack'

What can mathematics offer?

- biotissue highly viscoelastic and hysteretic
- acoustic shear waves caused by stenotic wake disturbance travel at frequency-dependent speed
- 150–750 Hz signals detectable at chest surface
- Exploit this for non-invasive computational diagnosis of arterial stenosis via inverse problem
- Challenging and ambitious: at a very early stage. . .

Localised disturbance: illustrative experiment. . .

Blood mimicking fluid pumped through artificially stenosed tube constrained within a TMM block (blue, forward; red, reversed).

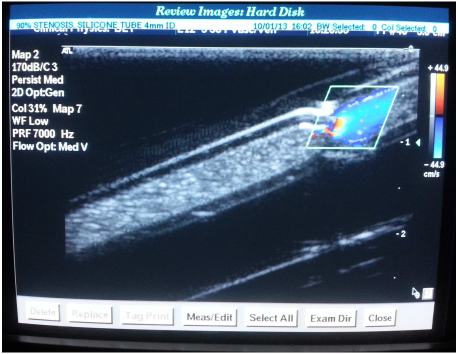

Localised disturbance: illustrative experiment. . .

Blood mimicking fluid pumped through artificially stenosed tube constrained within a TMM block (blue, forward; red, reversed).

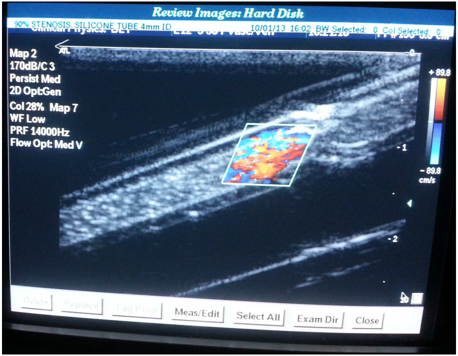

Localised disturbance: illustrative experiment. . .

Blood mimicking fluid pumped through artificially stenosed tube constrained within a TMM block (blue, forward; red, reversed).

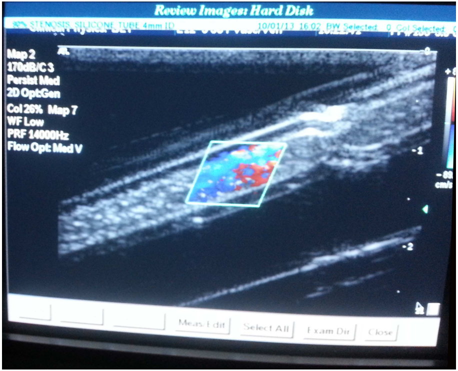

Localised disturbance: illustrative experiment. . .

Blood mimicking fluid pumped through artificially stenosed tube constrained within a TMM block (blue, forward; red, reversed).

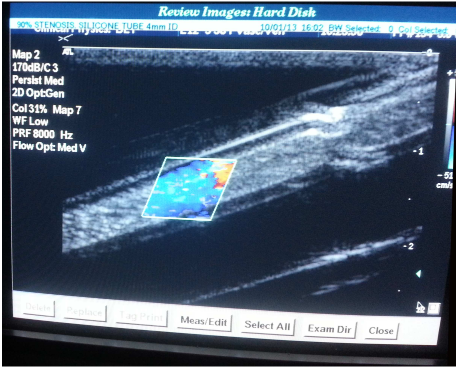

Localised disturbance: illustrative experiment. . .

Blood mimicking fluid pumped through artificially stenosed tube constrained within a TMM block (blue, forward; red, reversed).

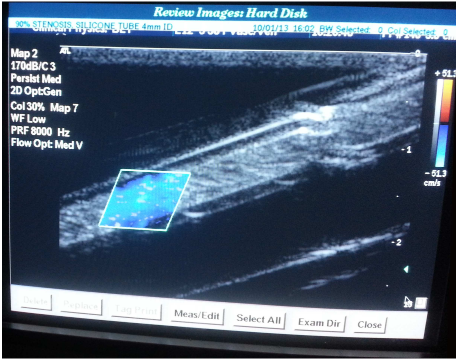

Localised disturbance: illustrative experiment. . .

Blood mimicking fluid pumped through artificially stenosed tube constrained within a TMM block (blue, forward; red, reversed).

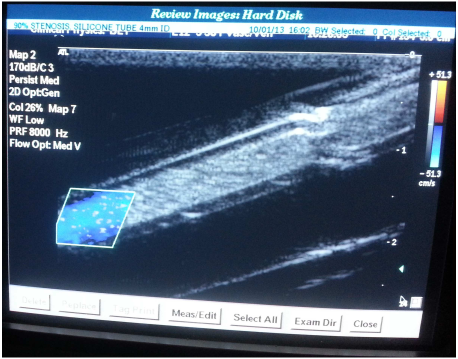

Semmlow and Rahalkar, Ann. Rev. Biomed. Eng. 2007 9:449–69

Acoustic Detection of Coronary Artery Disease

John Semmlow[1] and Ketaki Rahalkar[2]

[1]Robert Wood Johnson Medical School, Rutgers University, Piscataway, New Jersey 08854; email: Semmlow@biomed.rutgers.edu

[2]Department of Biomedical Engineering, Rutgers University, Piscataway, New Jersey 08854; email: ketaki_kholkute@yahoo.com

Annu. Rev. Biomed. Eng. 2007. 9:449–69

First published online as a Review in Advance on April 10, 2007

The *Annual Review of Biomedical Engineering* is online at bioeng.annualreviews.org

This article's doi: 10.1146/annurev.bioeng.9.060906.151840

1523-9829/07/0815-0449$20.00

Key Words

phonocardiography, heart sounds, coronary stenosis, coronary bruits, signal processing, cardiac microphones

Abstract

Coronary artery disease (CAD) occurs when the arteries to the heart (the coronary arteries) become blocked by deposition of plaque, depriving the heart of oxygen-bearing blood. This disease is arguably the most important fatal disease in industrialized countries, causing one-third to one-half of all deaths in persons between the ages of 35 and 64 in the United States. Despite the fact that early detection of CAD allows for successful and cost-effective treatment of the disease,

Semmlow and Rahalkar, Ann. Rev. Biomed. Eng. 2007 9:449–69

Coronary Artery Disease

John Semmlow[1] and Ketaki Rahalkar[2]

[1]Robert Wood Johnson Medical School, Rutgers University, Piscataway, New Jersey 08854; email: Semmlow@biomed.rutgers.edu

[2]Department of Biomedical Engineering, Rutgers University, Piscataway, New Jersey 08854; email: ketaki_kholkute@yahoo.com

Annu. Rev. Biomed. Eng. 2007. 9:449–69

First published online as a Review in Advance on April 10, 2007

The *Annual Review of Biomedical Engineering* is online at bioeng.annualreviews.org

This article's doi:
10.1146/annurev.bioeng.9.060906.151840

1523-9829/07/0815-0449$20.00

Key Words

phonocardiography, heart sounds, coronary stenosis, coronary bruits, signal processing, cardiac microphones

Abstract

Coronary artery disease (CAD) occurs when the arteries to the heart (the coronary arteries) become blocked by deposition of plaque, depriving the heart of oxygen-bearing blood. This disease is arguably the most important fatal disease in industrialized countries, causing one-third to one-half of all deaths in persons between the ages of 35 and 64 in the United States. Despite the fact that early detection of CAD allows for successful and cost-effective treatment of the disease,

Semmlow and Rahalkar, Ann. Rev. Biomed. Eng. 2007 9:449–69

John Semmlow[1] and Ketaki Rahalkar[2]

[1]Robert Wood Johnson Medical School, Rutgers University, Piscataway, New Jersey 08854; email: Semmlow@biomed.rutgers.edu

[2]Department of Biomedical Engineering, Rutgers University, Piscataway, New Jersey 08854; email: ketaki_kholkute@yahoo.com

. Rev. Biomed. Eng. 2007. 9:449–69

published online as a Review in Advance on
10, 2007

Annual Review of Biomedical Engineering is
e at bioeng.annualreviews.org

article's doi:
46/annurev.bioeng.9.060906.151840

-9829/07/0815-0449$20.00

Key Words

phonocardiography, heart sounds, coronary stenosis, coronary bruits, signal processing, cardiac microphones

Abstract

Coronary artery disease (CAD) occurs when the arteries to the heart (the coronary arteries) become blocked by deposition of plaque, depriving the heart of oxygen-bearing blood. This disease is arguably the most important fatal disease in industrialized countries, causing one-third to one-half of all deaths in persons between the ages of 35 and 64 in the United States. Despite the fact that early detection of CAD allows for successful and cost-effective treatment of the disease,

Semmlow and Rahalkar, Ann. Rev. Biomed. Eng. 2007 9:449–69

ned. Eng. 2007. 9:449–69

online as a Review in Advance on

iew of Biomedical Engineering is
.annualreviews.org

i:
v.bioeng.9.060906.151840

815-0449$20.00

Key Words

phonocardiography, heart sounds, coronary stenosis, coronary bruits, signal processing, cardiac microphones

Abstract

Coronary artery disease (CAD) occurs when the arteries to the heart (the coronary arteries) become blocked by deposition of plaque, depriving the heart of oxygen-bearing blood. This disease is arguably the most important fatal disease in industrialized countries, causing one-third to one-half of all deaths in persons between the ages of 35 and 64 in the United States. Despite the fact that early detection of CAD allows for successful and cost-effective treatment of the disease, only 20% of CAD cases are diagnosed prior to a heart attack. The development of a definitive, noninvasive test for detection of coronary blockages is one of the holy grails of diagnostic cardiology. One promising approach to detecting coronary blockages noninvasively

Semmlow and Rahalkar, Ann. Rev. Biomed. Eng. 2007 9:449–69

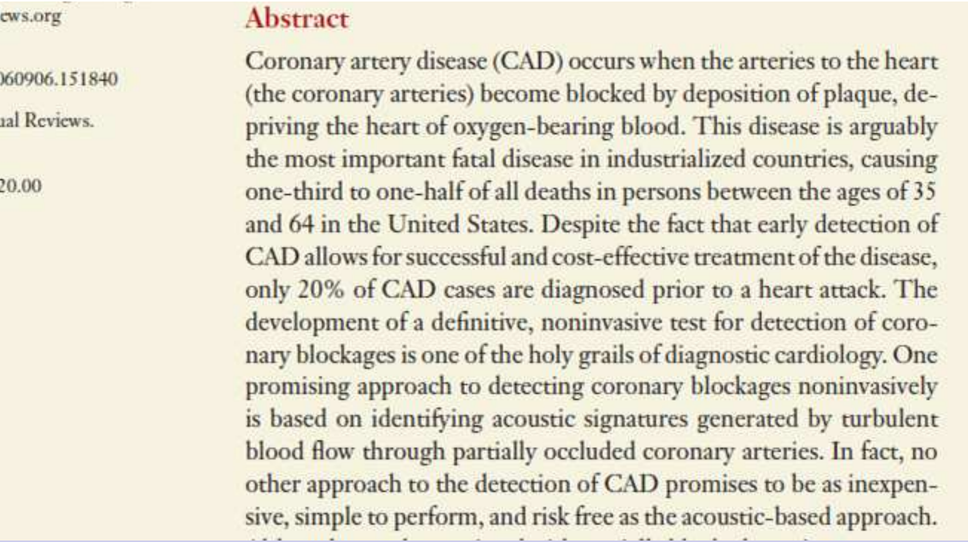
ews.org

)60906.151840

ıal Reviews.

20.00

Abstract

Coronary artery disease (CAD) occurs when the arteries to the heart (the coronary arteries) become blocked by deposition of plaque, depriving the heart of oxygen-bearing blood. This disease is arguably the most important fatal disease in industrialized countries, causing one-third to one-half of all deaths in persons between the ages of 35 and 64 in the United States. Despite the fact that early detection of CAD allows for successful and cost-effective treatment of the disease, only 20% of CAD cases are diagnosed prior to a heart attack. The development of a definitive, noninvasive test for detection of coronary blockages is one of the holy grails of diagnostic cardiology. One promising approach to detecting coronary blockages noninvasively is based on identifying acoustic signatures generated by turbulent blood flow through partially occluded coronary arteries. In fact, no other approach to the detection of CAD promises to be as inexpensive, simple to perform, and risk free as the acoustic-based approach.

Semmlow and Rahalkar, Ann. Rev. Biomed. Eng. 2007 9:449–69

one-third to one-half of all deaths in persons between the ages of 35 and 64 in the United States. Despite the fact that early detection of CAD allows for successful and cost-effective treatment of the disease, only 20% of CAD cases are diagnosed prior to a heart attack. The development of a definitive, noninvasive test for detection of coronary blockages is one of the holy grails of diagnostic cardiology. One promising approach to detecting coronary blockages noninvasively is based on identifying acoustic signatures generated by turbulent blood flow through partially occluded coronary arteries. In fact, no other approach to the detection of CAD promises to be as inexpensive, simple to perform, and risk free as the acoustic-based approach. Although sounds associated with partially blocked arteries are easy to identify in more superficial vessels such as the carotids, sounds from coronary arteries are very faint and surrounded by noise such as the very loud valve sounds. To detect these very weak signals requires

Semmlow and Rahalkar, Ann. Rev. Biomed. Eng. 2007 9:449–69

and 64 in the United States. Despite the fact that early detection of CAD allows for successful and cost-effective treatment of the disease, only 20% of CAD cases are diagnosed prior to a heart attack. The development of a definitive, noninvasive test for detection of coronary blockages is one of the holy grails of diagnostic cardiology. One promising approach to detecting coronary blockages noninvasively is based on identifying acoustic signatures generated by turbulent blood flow through partially occluded coronary arteries. In fact, no other approach to the detection of CAD promises to be as inexpensive, simple to perform, and risk free as the acoustic-based approach. Although sounds associated with partially blocked arteries are easy to identify in more superficial vessels such as the carotids, sounds from coronary arteries are very faint and surrounded by noise such as the very loud valve sounds. To detect these very weak signals requires sophisticated signal processing techniques. This review describes the

Semmlow and Rahalkar, Ann. Rev. Biomed. Eng. 2007 9:449–69

and 64 in the United States. Despite the fact that early detection of CAD allows for successful and cost-effective treatment of the disease, only 20% of CAD cases are diagnosed prior to a heart attack. The development of a definitive, noninvasive test for detection of coronary blockages is one of the holy grails of diagnostic cardiology. One promising approach to detecting coronary blockages noninvasively is based on identifying acoustic signatures generated by turbulent blood flow through partially occluded coronary arteries. In fact, no other approach to the detection of CAD promises to be as inexpensive, simple to perform, and risk free as the acoustic-based approach. Although sounds associated with partially blocked arteries are easy to identify in more superficial vessels such as the carotids, sounds from coronary arteries are very faint and surrounded by noise such as the

Semmlow and Rahalkar, Ann. Rev. Biomed. Eng. 2007 9:449–69

Key Finding. . .

no other approach . . . promises to be as inexpensive, simple. . . and risk free

What can computational mathematics offer?

Scoping/Feasibility Project: Methods and Aims

- Use the signature chest surface signal for screening and diagnosis. (Expected range $\sim 150\,\mathrm{Hz}$ — $750\,\mathrm{Hz}$.)
- *In vitro* biomechanics:
  - Characterize tissue mimicking agarose gel.
  - Build gel chest phantoms with controllable 'stenoses'.
  - Use a fluid loaded model to create shear waves.
- Computational Mathematics:
  - Material characterization through inverse problem data-fitting.
  - Simulations of wave transit through mimicked chest.
  - Stenosis localization through inverse solver.

EVENTUAL AIM
noninvasive screening & diagnosis

Acoustic Localisation of CAD

back

EPSRC
Engineering and Physical Sciences Research Council

Acoustic Localisation of Coronary Artery Stenosis

Brunel: EP/H011072/1
Queen Mary: EP/H011285/1
April 2010 — March 2014

Speculative Research

Multidisciplinary/international:

- Blizard (Queen Mary): chest phantom construction and experiments
- CRSC (North Carolina State): identification and inverse problem
- BICOM (Brunel): FE models & computation of direct problem

People: C Kruse, JR Whiteman, SE Greenwald, MJ Birch, MP Brewin, J Reeves, HT Banks, ZR Kenz, S Hu, B Kehra, E Cantor, D Mehta, I Gnaneswaren, S Shaw

Schematics - first steps

The reality. . .

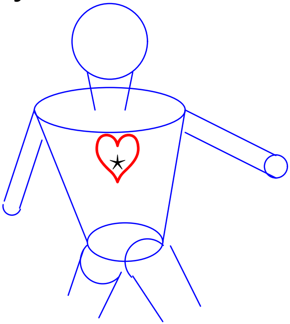

2D idealization

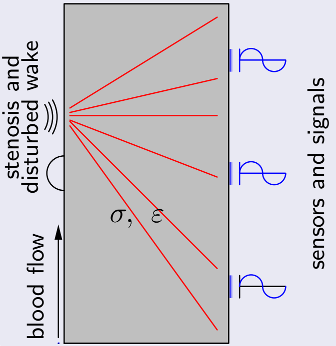

Schematics - first steps

The reality...

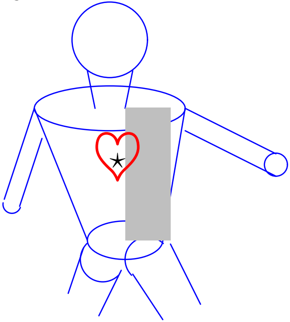

2D idealization

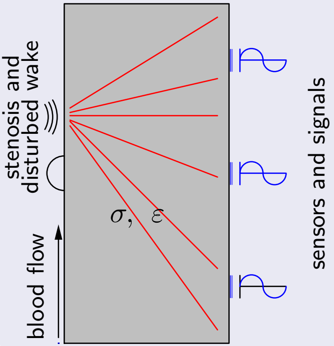

Schematics - first steps

The reality. . .

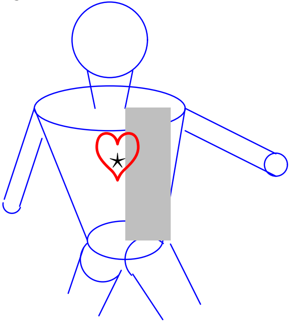

Proof of Concept: Agar Gel Chest Phantom

2D idealization

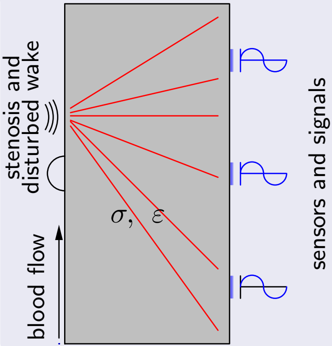

2D is computationally tractable at this early stage

Length scales of interest

Vertical chest cross section.

10cm (approx)

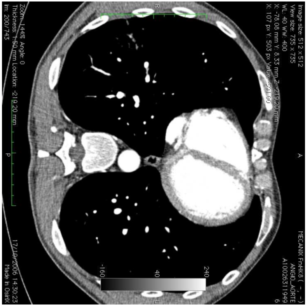

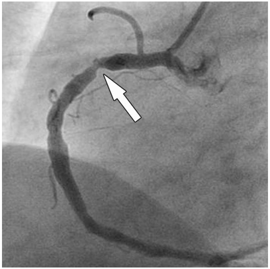

Reproduced with permission

Figure 4b from Baumüller S, Leschka S, Desbiolles L, et al. Dual-source versus 64-section CT coronary angiography at lower heart rates: comparison of accuracy and radiation dose. Radiology 2009;253:56-64. (c) RSNA 2009

Length scales of interest

Vertical chest cross section.

10cm (approx)

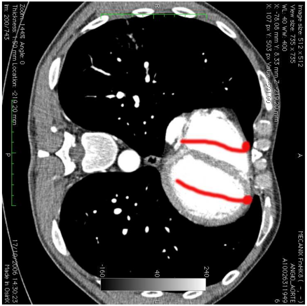

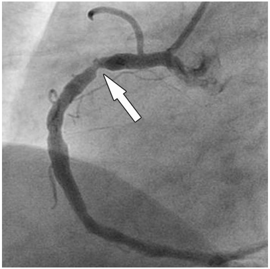

Reproduced with permission

Figure 4b from Baumüller S, Leschka S, Desbiolles L, et al. Dual-source versus 64-section CT coronary angiography at lower heart rates: comparison of accuracy and radiation dose. Radiology 2009;253:56-64. (c) RSNA 2009

The initial 2D rig – small scale at first

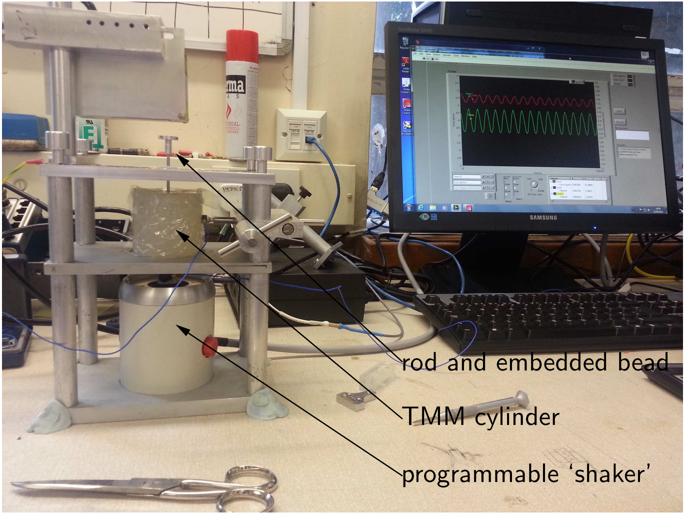

The mathematical model — classical linear viscodynamics

$$\varrho\dot{\boldsymbol{w}} - \nabla\cdot\underline{\boldsymbol{\sigma}} = \varrho\boldsymbol{f} \quad + \text{ initial and boundary data,}$$

with $\boldsymbol{w} = \dot{\boldsymbol{u}}$ and constitutive relationship,

$$\underline{\boldsymbol{\sigma}}(t) = \underbrace{\underline{\boldsymbol{C}}\underline{\boldsymbol{\varepsilon}}(\boldsymbol{w}(t))}_{\text{Voigt}} + \underbrace{\underline{\boldsymbol{D}}\underline{\boldsymbol{\varepsilon}}(\boldsymbol{u}(t))}_{\text{Hooke}} + \underline{\boldsymbol{D}} \underbrace{\int_0^t \varphi'(t-s)\underline{\boldsymbol{\varepsilon}}(\boldsymbol{u}(s))\,ds}_{\text{Maxwell/Zener}}$$

or internal variables for the Maxwell/Zener term,

$$\boldsymbol{z}_q(t) := \int_0^t \frac{\varphi_q}{\tau_q} e^{-(t-s)/\tau_q}\boldsymbol{u}(s)\,ds$$

Linearity!!!! Why? Justifiable? If not then is there any chance? ...

Current status

◂ back

Using the gel cylinder pictured earlier and the three outputs...

Assumptions

- For tensors $\underline{\boldsymbol{C}}$ and $\underline{\boldsymbol{D}}$ we take as a constitutive law,

$$\underline{\boldsymbol{\sigma}}(t) = \underbrace{\underline{\boldsymbol{C}}\underline{\boldsymbol{\varepsilon}}(\dot{\boldsymbol{u}}(t))}_{\text{Voigt}} + \underbrace{\underline{\boldsymbol{D}}\underline{\boldsymbol{\varepsilon}}(\boldsymbol{u}(t))}_{\text{Hooke}} + \underline{\boldsymbol{D}} \underbrace{\int_0^t \varphi'(t-s)\underline{\boldsymbol{\varepsilon}}(\boldsymbol{u}(s))\, ds}_{\text{Maxwell/Zener}}.$$

- We assume perfect knowledge of material data by experiments (QMUL/BLT) & inverse problems (CRSC): $E_0 = 229,389\,\mathrm{Pa}$, $\nu = 0.44$, $E_1 = 55,284\,\mathrm{Pa}\cdot\mathrm{s}$, $G_1 = 3.51\,\mathrm{Pa}\cdot\mathrm{s}$, $\varphi(t) = 1$ and $\varrho = 1010\,\mathrm{kg/m^3}$ on the meridian domain: $(0.175, 2.7)\,\mathrm{cm} \times (0, 5.1)\,\mathrm{cm}$.
- We allow additive/multiplicative Gaussian noise on the signals.

Current progress on the localisation problem

Use: gel cylinder, embedded vibrator and three surface outputs...

Algorithm

- A ramped-up sinusoidal $500\,\mathrm{Hz}$ axial-displacement source is placed at a known position $\bar{z}$ in the central bore.
- The forward solver computes the axial displacement surface signal at heights $13\,\mathrm{mm}$, $26\,\mathrm{mm}$ and $39\,\mathrm{mm}$.
- These 'truth' data are 'banked' and may or may not be deliberately corrupted with additive noise: noisy truth $=$ truth $+ N_L \times \epsilon$ for N_L a noise level amplitude and $\epsilon \sim N(0,1)$. (Or with multiplicative noise.)
- The position of the source $\bar{z}$ is now 'forgotten'.
- `matlab`'s `fminsearch` iteratively estimates $\bar{z}$ given only the (noisy) truth and the forward solve outputs

Forward solver: Bicubic Galerkin finite elements were used on a 25×51 element mesh and with $24,000$ Crank-Nicolson time steps for $0 \leqslant t \leqslant 1\,\mathrm{s}$.

Some results for a $500\,\mathrm{Hz}$ source signal.

Assume perfect knowledge of material constants.

Examples of a 'true' signal and a corrupted version: additive Gaussian noise, amplitude 10^{-6}.

True Signal

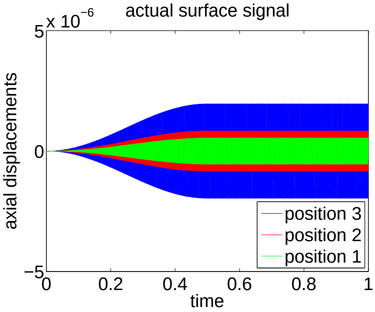

Corrupted Signal

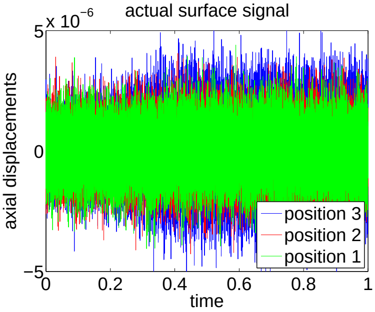

Example: $500\,\mathrm{Hz}$ with 10^{-6} noise

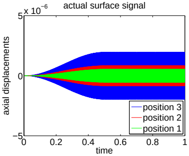

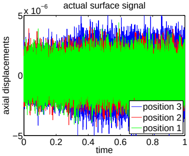

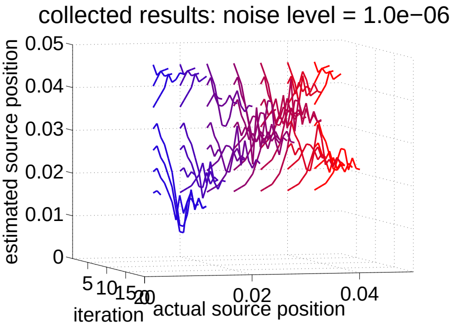

Well posed-ness seems to follow from a good starting value.
Some robustness in the presence of significant measurement noise.

Summary: $500\,\mathrm{Hz}$ with 10^{-6} noise

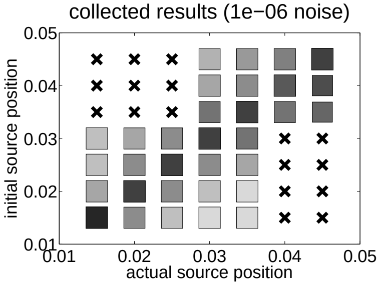

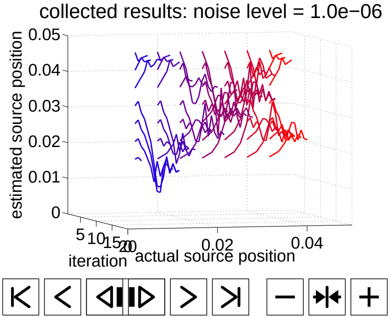

Well posed-ness seems to follow from a good starting value.
Some robustness in the presence of significant measurement noise.

Comparison: $500\,\mathrm{Hz}$ no noise (left) 10^{-6} noise (right)

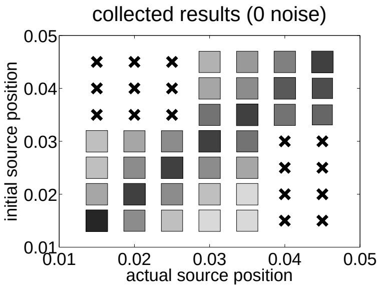

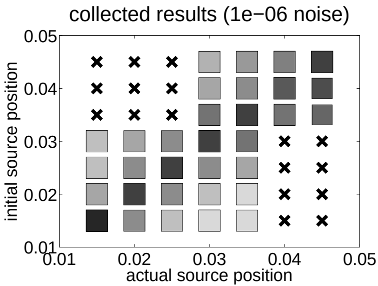

Square indicate success: darker shades mean fewer iterations.

Crosses represent failure.

Comparison: $500\,\mathrm{Hz}$
hi-fi and noiseless (left), lo-fi with 10^{-6} noise (right)

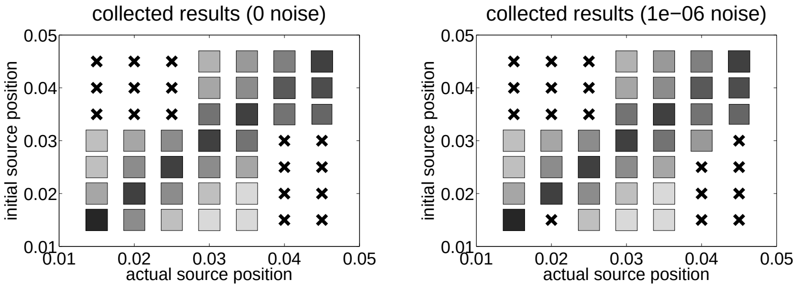

Left: 25×51 mesh of bicubics, 24000 time steps

Right: 25×51 mesh of bilinears, 12000 time steps

The story so far, and what comes next

back

- Little change of performance with lo-fi forward solves and very significant additive and multiplicative Gaussian signal-noise.
- Reasonably good initial guesses lead to correct localisation: end effects seem a problem.
- Each localization problem needs about 12 hours: need parallelism, further optimized code, . . .
- Next step is to build and simulate a 3D virtual chest with phantom ribs, lungs, heart, arteries, skin and fat.

High Order DG-in-time FEM

back

High Order Space-Time FEM for Wave Equations

back

Space-Time Finite Elements

High order numerical schemes are known for. . .

- smaller dispersion error in wave propagation problems
- better work/accuracy ratios

We've developed temporally high order time-diagonalised space-time finite element codes for elasto- and visco-dynamics.

We use continuous spectral (i.e. Galerkin with Gauss-Lobatto) FEM in space and discontinuous Galerkin in time. jump

We can compute easily using fifth-degree space-time polynomial approximations.

Hi-Fi solutions are not necessarily important for inverse solvers but speed/parallelism is. . .

Discretize a wave equation in time with DGFEM: for each $n = 1, 2, \ldots, N$ in turn, find $(U, W)|_{I_n} \in \mathbb{P}_r(I_n; V) \times \mathbb{P}_r(I_n; V)$ such that

$$\int_{I_n} (\dot{W}(t), \vartheta(t)) + a(U(t), \vartheta(t))\, dt + ([\![W]\!]_{n-1}, \vartheta^+_{n-1}) + a([\![U]\!]_{n-1}, \zeta^+_{n-1})$$

$$+ \int_{I_n} a(\dot{U}(t), \zeta(t)) - a(W(t), \zeta(t))\, dt = \int_{I_n} \langle L(t), \vartheta(t)\rangle\, dt$$

$$\forall \vartheta \in \mathbb{P}_r(I_n; V) \quad \text{and} \quad \forall \zeta \in \mathbb{P}_r(I_n; V),$$

with IC's: $U_0^- := \breve{u}$ and $W_0^- := \breve{w}$; and $\mathbb{P}_r(I_n; X)$ the space of polynomials of degree r on the time interval I_n with coefficients in the target space X. Note that r could be n-dependent.

Diagonalize following: Werder, Gerdes, Schötzau and Schwab, CMAME 2001; 190:6685—6708.

…then gives the decoupled form,

$$\begin{aligned} 2\lambda_i(Y_i,\vartheta) + k_n a(Z_i,\vartheta) &= 2F_i(\vartheta), \\ a(2\lambda_i Z_i - k_n Y_i,\vartheta) &= 2\beta_i a(U_{n-1}^-,\vartheta) \end{aligned}$$

for $i = 0, 1, 2, \ldots, r =$ the temporal polynomial degree.

This complex symmetric system requires just one matrix solve for each pair (Y_i, Z_i) and (U, W) are recovered from them.

In IJNME 2014, 98:131156 (DOI: 10.1002/nme.4631), we showed that expected convergence rates are obtained for temporal polynomial degrees up to seven.

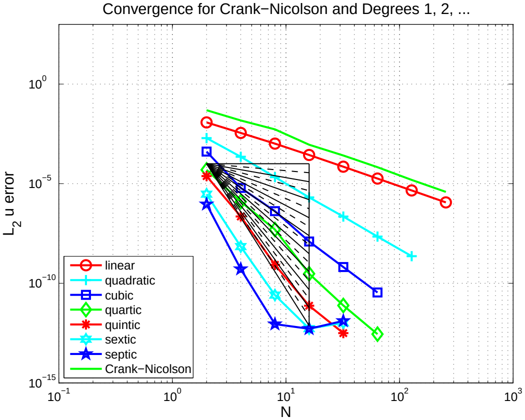

In IJNME 2014; 98:131156 (DOI: 10.1002/nme.4631) we showed that expected convergence rates are obtained for temporal polynomial degrees up to seven.

back

Spectral FE for CG-in-time heat equation

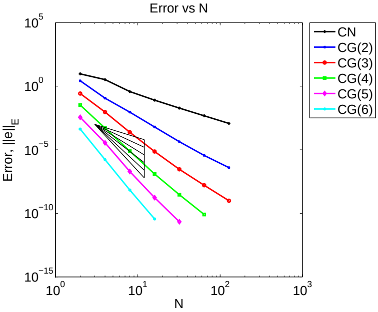

Using Gauss-Lobatto for time integration...

In SISC, 36:B1B13 (DOI: 10.1137/130914589), we showed that expected convergence rates are obtained for temporal polynomial degrees up to six.

Lots to do/test

This is to some extent empirical. Unclear how it deals with

- variable coefficients
- nonlinearities
- dispersion error
- singularities

But it is suited to the coming many-core era...

And one can imagine several variant schemes.

BRUNEL MAFELAP 2016

The fifteenth conference on

The Mathematics of Finite Elements and Applications 2016

14 - 17 June 2016

Over 330 participants in 2013.

Mini-Symposia proposals welcomed.

registration is open.

A last thought

$$\nabla^2\phi = 0 \qquad {}_{H'}\langle F, v\rangle_H = (f,v)_H \quad \forall v\in H \qquad z \leftarrow z^2 + c \qquad \nabla\times E + \dot{B} = 0$$

$$u_t + u\cdot\nabla u = \frac{1}{\rho}\nabla p + \mu\nabla^2 u \qquad \frac{\partial C}{\partial t} + \frac{\sigma^2 S^2}{2}\frac{\partial^2 C}{\partial S^2} + rS\frac{\partial C}{\partial S} = rC \qquad \ddot{u} = c^2\nabla^2 u$$

$$V_t = e^{-r(T-t)}\mathbb{E}_Q(X|\mathcal{F}_t) \qquad x_{n+1} = x_n - \frac{f(x_n)}{f'(x_n)} \qquad -\sigma_{ij,j} = f_i \qquad (uv)' = uv' + u'v$$

$$\varepsilon(u) := \frac{1}{2}\left(\frac{\partial u_i}{\partial x_j} + \frac{\partial u_j}{\partial x_i}\right) \qquad Av = \lambda v \qquad i\hbar\frac{\partial\psi}{\partial t} = -\frac{\hbar}{2m}\nabla^2\psi + V\psi$$

$$a(u,v) = f(v) \quad \forall v\in \mathring{H}^1(\Omega) \qquad \phi(y) = \psi(y) + \int_\Omega \kappa(y-x)z(x)\phi(x)\,dx$$

$$\frac{dy}{dx} = \frac{dy}{du}\frac{du}{dv}\frac{dv}{dx} \qquad \frac{1}{\sqrt{2\pi\sigma^2}}\exp\left(-\frac{(x-\mu)^2}{2\sigma^2}\right) \qquad \frac{\partial u}{\partial t} - \nabla^2 u = 0$$

$$\nabla\times H - \dot{D} = J \qquad \frac{dS}{S} = \mu dt + \sigma dX \qquad f(z_0) = \frac{1}{2\pi i}\int_\gamma \frac{f(z)}{z-z_0}\,dz$$

$$dG = \left(a\frac{\partial G}{\partial \ldots}\right) \qquad \frac{v\frac{du}{dx} - u\frac{dv}{dx}}{v^2}$$

A last thought

$\nabla^2\phi = 0 \quad {}_{H'}\langle F, v\rangle_H = (f, v)_H \quad \forall v \in H \quad z \leftarrow z^2 + c \quad \nabla \times E + \dot{B} = 0$

The difference between theory and practice in practice
is greater than
the difference between theory and practice in theory

Yogi Berra, Albert Einstein, ...

$\nabla \times H - \dot{D} = J \quad \frac{dS}{S} = \mu dt + \sigma dX \quad f(z_0) = \frac{1}{2\pi i}\int_\gamma \frac{f(z)}{z - z_0}\,dz$

A last thought

$\nabla^2\phi = 0 \quad {}_{H'}\langle F, v\rangle_H = (f, v)_H \quad \forall v \in H \quad z \leftarrow z^2 + c \quad \nabla \times E + \dot{B} = 0$

The difference between theory and practice in practice
is greater than
the difference between theory and practice in theory

Yogi Berra, Albert Einstein, ...

Thank You For Listening

$\nabla \times H - \dot{D} = J \quad \frac{dS}{S} = \mu dt + \sigma dX \quad f(z_0) = \frac{1}{2\pi i}\int_\gamma \frac{f(z)}{z - z_0}\,dz$

Appendix — time permitting

Time Diagonalisation

back

Consider a generic wave equation in weak form: find $u\colon L_2(0,T) \to V$ such that

$$\int_{I_n} (\dot{w}(t), v(t)) + a(u(t), v(t))\, dt = \int_{I_n} \langle L(t), v(t)\rangle\, dt \quad \forall v \in L_2(0,T;V).$$

where: $I_n = (t_{n-1}, t_n)$, $w = \dot{u}$, V is a Hilbert space, $a\colon V \times V \to \mathbb{R}$ a symmetric bilinear form and $L\colon L_2(0,T) \to V'$ a time dependent linear form containing body loads and boundary tractions.

Discretize in time using Discontinuous Galerkin finite elements...

Discretize in time with DGFEM: for each $n = 1, 2, \dots, N$ in turn, find $(U, W)|_{I_n} \in \mathbb{P}_r(I_n; V) \times \mathbb{P}_r(I_n; V)$ such that

$$\int_{I_n} (\dot{W}(t), \vartheta(t)) + a(U(t), \vartheta(t))\, dt + ([\![W]\!]_{n-1}, \vartheta^+_{n-1}) + a([\![U]\!]_{n-1}, \zeta^+_{n-1})$$
$$+ \int_{I_n} a(\dot{U}(t), \zeta(t)) - a(W(t), \zeta(t))\, dt = \int_{I_n} \langle L(t), \vartheta(t)\rangle\, dt$$
$$\forall \vartheta \in \mathbb{P}_r(I_n; V) \quad \text{and} \quad \forall \zeta \in \mathbb{P}_r(I_n; V),$$

with the understanding that the initial conditions are $U_0^- := \breve{u}$ and $W_0^- := \breve{w}$. Here, for each n, we use $\mathbb{P}_r(I_n; X)$ to denote the space of polynomials of degree r on the time interval I_n with coefficients in the target space X. Note that r could be n-dependent.

Diagonalize following: Werder, Gerdes, Schötzau and Schwab, CMAME 2001; 190:6685—6708.

$$\int_{I_n} (\dot{W}(t), \vartheta(t)) + a(U(t), \vartheta(t))\, dt + ([\![W]\!]_{n-1}, \vartheta_{n-1}^{+}) + a([\![U]\!]_{n-1}, \zeta_{n-1}^{+})$$
$$+ \int_{I_n} a(\dot{U}(t), \zeta(t)) - a(W(t), \zeta(t))\, dt = \int_{I_n} \langle L(t), \vartheta(t)\rangle\, dt$$
$$\forall \vartheta \in \mathbb{P}_r(I_n; V) \quad \text{and} \quad \forall \zeta \in \mathbb{P}_r(I_n; V),$$

Let $\{\phi_i : i = 0, 1, \ldots, r\}$ be a basis for $\mathbb{P}_r(I_n)$ and introduce the ansatz forms of the approximations to u and w on I_n as,

$$U(t)|_{I_n} = \sum_{j=0}^{r} \phi_j(t) U_j \qquad \text{and} \qquad W(t)|_{I_n} = \sum_{j=0}^{r} \phi_j(t) W_j$$

where $\{U_0, U_1, \ldots\}, \{W_0, W_1, \ldots\} \subseteq V$. Replacing each of $\vartheta(t)$ and $\zeta(t)$ with $\phi_i(t)\vartheta$ for $\phi_i \in \mathbb{P}_r(I_n)$ and $\vartheta \in V$ we obtain...

$$\sum_{j=0}^{r}\int_{I_n}\dot{\phi}_j(t)\phi_i(t)(W_j,\vartheta)+\phi_j(t)\phi_i(t)a(U_j,\vartheta)\,dt$$
$$+\sum_{j=0}^{r}\phi_{j,n-1}^{+}\phi_{i,n-1}^{+}(W_j,\vartheta)=\int_{I_n}\phi_i(t)\langle L(t),\vartheta\rangle\,dt+\phi_{i,n-1}^{+}(W_{n-1}^{-},\vartheta)$$

and,

$$\sum_{j=0}^{r}\int_{I_n}\dot{\phi}_j(t)\phi_i(t)a(U_j,\vartheta)-\phi_j(t)\phi_i(t)a(W_j,\vartheta)\,dt$$
$$+\sum_{j=0}^{r}\phi_{j,n-1}^{+}\phi_{i,n-1}^{+}a(U_j,\vartheta)=\phi_{i,n-1}^{+}a(U_{n-1}^{-},\vartheta)$$

where each holds for all $\vartheta\in V$ and for each $i\in\{0,1,\ldots,r\}$.

Define matrices via,

$$\mathsf{A}_{ij} := \int_{I_n} \dot{\phi}_j(t)\phi_i(t)\,dt + \phi^+_{j,n-1}\phi^+_{i,n-1} \text{ and } \mathsf{M}_{ij} := \int_{I_n} \phi_j(t)\phi_i(t)\,dt,$$

where i indexes the rows. Choosing basis functions as the image under the linear map from $[-1, 1]$ to I_n of the normalized Legendre polynomials gives $2\mathsf{M} = k_n\mathsf{I}$ — diagonal!

A is diagonalizable over $\mathbb{C}$ for all polynomial degrees of practical interest ($r \leqslant 100$). Ref: Werder *et al.* CMAME 2001; 190:6685—6708.

In fact: $\mathsf{D} = \mathsf{Q}^{-1}\mathsf{A}\mathsf{Q} = \ulcorner \lambda_0 \cdots \lambda_r \lrcorner$ where $\ulcorner \cdots \lrcorner$ indicates a diagonal matrix of pairwise complex conjugate eigenvalues and where Q has complex entries.

Using the summation convention our system is:

$$\begin{aligned}\mathsf{A}_{ij}(W_j,\vartheta)+\delta_{ij}\frac{k_n}{2}a(U_j,\vartheta) &= \mathsf{F}_i(\vartheta),\\ \mathsf{A}_{ij}a(U_j,\vartheta)-\delta_{ij}\frac{k_n}{2}a(W_j,\vartheta) &= \mathsf{G}_i(\vartheta),\end{aligned}$$

where F_i and G_i contain known data.

Let $\{Y_q\}$ and $\{Z_q\}$ uniquely solve $W_j = \mathsf{Q}_{jq}Y_q$ and $U_j = \mathsf{Q}_{jq}Z_q$:

$$\begin{aligned}\mathsf{A}_{ij}\mathsf{Q}_{jq}(Y_q,\vartheta)+\delta_{ij}\frac{k_n}{2}\mathsf{Q}_{jq}a(Z_q,\vartheta) &= \mathsf{F}_i(\vartheta),\\ \mathsf{A}_{ij}\mathsf{Q}_{jq}a(Z_q,\vartheta)-\delta_{ij}\frac{k_n}{2}\mathsf{Q}_{jq}a(Y_q,\vartheta) &= \mathsf{G}_i(\vartheta),\end{aligned}$$

Premultiply with $\mathsf{R}=\mathsf{Q}^{-1}$, noting that,

$$\mathsf{R}_{pi}\mathsf{A}_{ij}\mathsf{Q}_{jq} = \delta_{pq}\lambda_p \text{ and } \mathsf{R}_{pi}\delta_{ij}\mathsf{Q}_{jq} = \delta_{pq},$$

and setting $F_i(\vartheta) := \mathsf{R}_{ip}\mathsf{F}_p(\vartheta)$ and $G_i(\vartheta) := \mathsf{R}_{ip}\mathsf{G}_p(\vartheta)$...

...then gives the decoupled form,

$$\begin{aligned} 2\lambda_i(Y_i,\vartheta) + k_n a(Z_i,\vartheta) &= 2F_i(\vartheta), \\ 2\lambda_i a(Z_i,\vartheta) - k_n a(Y_i,\vartheta) &= 2G_i(\vartheta) \end{aligned}$$

for $i = 0, 1, 2, \ldots, r =$ the temporal polynomial degree.

This complex symmetric system requires just one matrix solve.

In IJNME 2014, 98:131156 (DOI: 10.1002/nme.4631), we showed that expected convergence rates are obtained for temporal polynomial degrees up to seven.

back

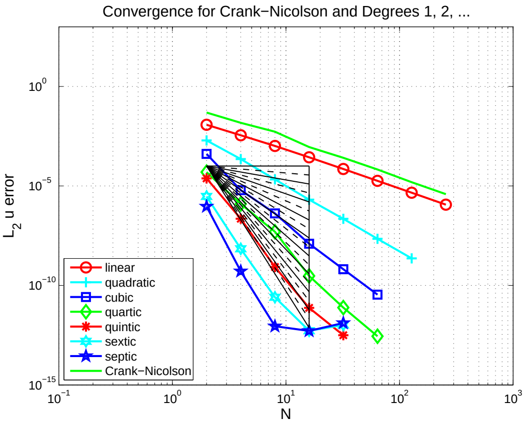

In IJNME 2014; 98:131156 (DOI: 10.1002/nme.4631) we showed that expected convergence rates are obtained for temporal polynomial degrees up to seven.

back

Spectral FE for CG-in-time heat equation

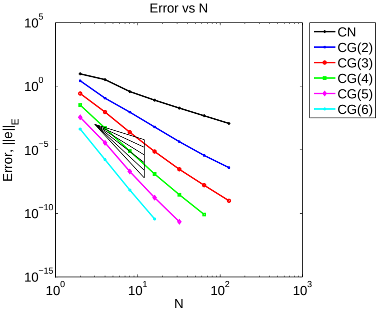

Using Gauss-Lobatto for time integration. . .

In SISC, 36:B1B13 (DOI: 10.1137/130914589), we showed that expected convergence rates are obtained for temporal polynomial degrees up to six.

back